but also on the reactivity of the charge-transfer excited triplet state of the catalyst toward O_2 and CO molecules.

Finally, it is worth mentioning that this information on the charge-transfer excited state of the metal oxides is very important to elucidate the true nature not only of the photoinduced and/or photocatalytic reactions but also of catalysis on the metal oxides, because it has been suggested that the charge-transfer excited state could also be obtained by thermal activation in the catalytic systems on metal oxides.[22,47,48]

Acknowledgment. M.A. is much indebted to Professor M. A. Fox of The University of Texas at Austin for helpful discussions. M.A. also thanks the Université P. et M. Curie for a position as invited Professor at Paris. This work has been partially supported by the Ministry of Education of Japan for Grant-in-Aid Scientific Research (Grant No. 62550595) and Grant-in-Aid for Special Project Research (Grant No. 61223022).

Registry No. Mo, 7439-98-7; O_2, 7782-44-7; CO, 630-08-0.

Dynamic Aspects of the Stereochemistry of Metalated Oxime Ethers. An ab Initio Study of the Pathways for Coordination Isomerization, for Syn/Anti Isomerization, and for Racemization of the Lithium Ion Pairs from Acetaldoxime[1]

Rainer Glaser[2] and Andrew Streitwieser*

Contribution from the Department of Chemistry, University of California, Berkeley, California 94720. *Received July 20, 1988*

Abstract: The pathways to isomerization between the chiral lithium ion pairs of acetaldoxime carbanion have been explored. The configuration of each ion pair is classified using two descriptors. In equilibrium structures one descriptor suffices to describe the configuration of each structure, but both descriptors are necessary for the recognition and consideration of all a priori possible pathways for racemization. Coordination isomerizations and racemizations of the syn- and the anti-configured ion pairs are discussed as special cases of the more general eight-minima scenario representing the epimers of two coordination isomers and their enantiomers, and the syn/anti isomerization is treated separately. This eight-minima scenario is described by a graph representation that reflects that the pathways for any pair of isomerizations $X \rightleftarrows Y$ and $X' \rightleftarrows Y'$ are enantiomerically related. Of all of the possible one-step isomerizations in this scenario only racemizations have the potential to involve achiral transition states since the enantiomerically related pathways $X \rightleftarrows X'$ might be identical. A systematic search for the transition-state structures for coordination isomerization and racemization is described on the basis of the symmetry properties of the imaginary vibrational modes of the achiral structures. Entirely chiral pathways for racemization exist if the corresponding achiral structure is a second-order saddle point and one of the imaginary modes fulfills the so-called IPD condition. The optimal geometries of all reasonable achiral structures have been characterized by vibrational normal mode analysis. In cases where the achiral structure is a second-order saddle point, the adjacent transition states have been located. The racemization of the η^2-NO-bond coordinated anti-configured ion pair involves entirely chiral pathways, but the potential energy surface in the bifurcating region is extremely flat. The syn/anti isomerization most likely involves rotation of the HO group around the CN axis, and the transition-state structure for this pathway has been located. All of these processes occur with only small barriers and should be facile. Thus, any of the structures is readily available as a reaction intermediate or as a building block for ion-pair aggregates. Mechanistic implications are discussed with regard to possible face selectivity of the electrophile entry. The small barrier to coordination isomerization has significant consequences for the design of strategies for regio- and stereoselective CC-bond formation at the α-carbon of diastereoisomeric metalated oxime ethers.

The introduction of metalated enolate equivalents by Wittig,[3] Stork,[4] and Hauser[5] resolved many of the problems associated with the classical methods for the regioselective formation[6] of a new carbon–carbon bond at the α-position of a carbonyl group. Metalated nitrogen derivatives of aldehydes and ketones have since become well established as an important class of intermediates in modern synthetic chemistry.[7,8] Metalated imines,[9–14] hydrazones,[15–19] and oxyimines[20–30] are typically generated by low-temperature deprotonation with a strong metalorganic base in

(1) Presented in part at the 194th National Meeting of the American Chemical Society, New Orleans, LA, Aug 30 – Sept 4, 1987, and at the 2nd International Conference on Theoretical Organic Chemistry, Budapest, Aug 10–16, 1987.

(2) Predoctoral Fellow of the Fonds der Chemischen Industrie, 1985–87. Current address: Department of Chemistry, University of Missouri–Columbia, College Ave., Columbia, MO 65211.

(3) (a) Wittig, G.; Frommeld, H. D.; Suchanek, P. *Angew. Chem.* **1963**, *75*, 978. (b) Wittig, G.; Reiff, H. *Angew. Chem.* **1968**, *80*, 8. (c) Wittig, G.; Hesse, A. *Org. Synth.* **1970**, *50*, 66.

(4) (a) Stork, G.; Dowd, S. R. *J. Am. Chem. Soc.* **1963**, *85*, 2178. (b) Stork, G.; Benaim, J. *J. Am. Chem. Soc.* **1971**, *93*, 5938. (c) Stork, G.; Dowd, S. R. *Org. Synth.* **1974**, *50*, 66.

(5) Henoch, F. E.; Hampton, K. G.; Hauser, C. R. *J. Am. Chem. Soc.* **1969**, *91*, 676.

(6) (a) Stork, G. *Pure Appl. Chem.* **1975**, *43*, 553. (b) D'Angelo, J. *Tetrahedron* **1976**, *32*, 2979.

(7) Reviews: (a) Hickmott, P. W. *Tetrahedron* **1982**, *14*, 1975. (b) Mukaiyama, T. *Pure Appl. Chem.* **1983**, *55*, 1749. (c) Evans, D. *Stereoselective Reactions of Chiral Metal Enolates.* In *Asymmetric Synthesis*; Morrison, J. D., Ed.; Academic Press: Orlando, FL, 1984; Vol. 3, p 1. (d) Enders, D. Alkylation of Chiral Hydrazones. In ref 7c, p 275.

(8) Reviews: (a) Fraser, R. R. *Stud. Org. Chem. (Amsterdam)* **1984**, *5B*, 65. (b) Gompper, P.; Vogt, H. H.; Wagner, H. U. *Z. Naturforsch.* **1981**, *36B*, 1644.

(9) (a) Ferran, H. E., Jr.; Roberts, R. D.; Jacob, J. N.; Spencer, T. A. *J. Chem. Soc., Chem. Commun.* **1978**, 49. (b) Lee, J. Y.; Lynch, T. J.; Mao, D. T.; Bergbreiter, D. E.; Newcomb, M. *J. Am. Chem. Soc.* **1981**, *103*, 6215.

(10) (a) Meyers, A. I.; Williams, D. R.; Druelinger, M. *J. Am. Chem. Soc.* **1976**, *98*, 3032. (b) Meyers, A. I.; Poindexter, G. S.; Brich, Z. *J. Org. Chem.* **1978**, *43*, 892. (c) Meyers, A. I.; Williams, D. R. *J. Org. Chem.* **1978**, *43*, 3245.

(11) Houk, K. N.; Strozier, R. W.; Rondan, N. G.; Fraser, R. R.; Chuaqui-Offermanns *J. Am. Chem. Soc.* **1980**, *102*, 1426.

(12) (a) Fraser, R. R.; Chuaqui-Offermanns, N.; Houk, H. N.; Rondan, N. G. *J. Organomet. Chem.* **1981**, *206*, 131. (b) Fraser, R. R.; Bresse, M.; Chuaqui-Offermanns, N.; Houk, K. N.; Rondan, N. G. *Can. J. Chem.* **1983**, *61*, 2729.

(13) Meyers, A. I.; Mihelich, E. D. *Angew. Chem., Int. Ed. Engl.* **1976**, *15*, 270.

0002-7863/89/1511-8799$01.50/0

solvents of low polarity. Reactions of these intermediates with electrophiles result generally in the products of the syn-configured intermediate in a highly regiospecific fashion.[7-31] This remarkable regiospecificity has also been exploited in carbon–carbon bond formations by oxidative addition of the enolate equivalents,[5,29] and, importantly, it provides the basis for stereospecific functionalization at the α-carbon of carbonyl compounds via N derivatives with chiral auxiliaries.[7]

Studies of the equilibrium structures of the reactive intermediates, of the energy differences between isomeric species, and of the activation barriers for isomerizations are pertinent to more fully understand the chemistry of these metalated enolate equivalents and to design novel synthetic strategies on this basis. To address such questions for reactions involving oxyimines such as oximes,[5,20-24] oxime ethers,[25-29] and oxazines,[30] we have studied the configurational and conformational preferences of oxime carbanions,[32] of oxime dianions,[33] and of mono- and dimetalated oximes[33-35] by ab initio techniques. The dianions and their dimetalated derivatives are discussed elsewhere.[33] The carbanions of oximes are models for enolate equivalents of oxime ethers and oxazines if the reaction conditions favor free ions.[32] Typically, reactions of metalated enolate equivalents are carried out in solvents of low polarity in which ion pairs or aggregates are the probable reactive species. We have previously reported the equilibrium geometries and relative isomer stabilities of monomeric ion pairs of oxime carbanions.[34,35] These studies have shown that the observed stereochemistry is consistent with the properties of the monomeric ion pairs and led us to propose that these ion pairs be considered in discussions of reaction mechanism of metalated oxime ethers.[35] Semiempirical calculations have shown that ion-pair aggregation may well be important in solution but that the monomeric ion pairs are the more likely reactive species.[36]

We now report dynamic aspects of the monomeric lithium ion pair of acetaldoxime. The equilibrium structures are discussed briefly, and each enantiomer is classified using two descriptors. While one descriptor suffices to fully characterize the minima on the potential energy surface, the analysis of an eight-minima scenario emphasizes that at least two descriptors are required for full consideration of the isomerization pathways. We show that racemizations of molecules with more than one basic element of chirality (vide infra) may involve entirely chiral pathways and that the recognition of all of the elements of chirality is sometimes obscured by nomenclature. We also describe how the search for the isomerization transition state structures can be facilitated with the information contained in the imaginary mode(s) of achiral stationary structures. Transition-state structures have been located for syn/anti isomerization as well as for racemization and coordination-isomerization pathways of the syn- and anti-configured ion pairs. All of these processes are important for the determination of the structure(s) of the reactive species and for the mechanism(s) of reactions with electrophiles. Implications of these theoretical results are discussed.

Table I. Energies and Vibrational Zero-Point Energies[a]

molecule[b]	symmetry	−energy[a] 3-21+G	−energy[a] 6-31+G*//3-21+G	ZPE[c]	CSS[d]
6a, C_1	*syn*-X^-Li^+	213.605 50	214.751 87	41.42	M
6b, C_1	*syn*-X^-Li^+	213.609 38	214.751 74	41.29	M
6c, C_s	*syn*-X^-Li^+	213.588 67	214.743 57	40.72	TS
6d, C_s	*syn*-X^-Li^+	213.577 51	214.726 37	41.07	TS
7a, C_1	*anti*-X^-Li^+	213.590 70	214.746 76	41.03	M
7b, C_1	*anti*-X^-Li^+	213.604 66	214.746 84	40.97	M
7c, C_s	*anti*-X^-Li^+	213.571 98	214.733 54	40.10	TS
7d, C_s	*anti*-X^-Li^+	213.578 97	214.727 79	40.22	SOSP
7e, C_s	*anti*-X^-Li^+	213.597 31	214.735 80	39.91	SOSP
7f, C_1	*anti*-X^-Li^+	213.581 17	214.734 39	40.54	TS
7g, C_1	*anti*-X^-Li^+	213.597 31	214.735 75	39.94	TS
11, C_1	X^-Li^+	213.591 38	214.730 19	40.57	TS

[a] Energies (−*E*, in atomic units) and vibrational zero-point energies in kcal mol^{-1}. [b] $HONCHCH_2^-$ = X^-. [c] Unscaled. [d] Character of stationary structure: M = minimum, TS = transition state (first-order saddle point), and SOSP = second-order saddle point.

Computational Aspects

Standard restricted Hartree–Fock calculations were carried out with the programs[37] GAUSSIAN 80 and GAUSSIAN 82. Geometries were optimized with analytical gradient techniques[38] under the constraints of the symmetry point group specified. As in our previous studies,[34,35] the 3-21G basis set[39] was used for lithium and the anions in the ion pairs were described with the 3-21+G basis set.[40,41] This choice of basis set, denoted 3-21+G, despite the modest modification, provides a more balanced functional description of the paired ions.[42] Harmonic vibrational frequencies were calculated at the level of optimization to characterize stationary points as minima or saddle points and to obtain vibrational zero-point energies. The vibrational zero-point energy corrections to relative energies were scaled (factor 0.9) to take account of their usual overestimation at this computational level.[43] Energies were calculated with these geometries and a slightly altered 6-31G* basis set.[44] The standard 6-31G* basis set was modified in that no d-functions were used

(14) Whitesell, J. K.; Whitesell, M. A. *J. Org. Chem.* **1977**, *42*, 377.
(15) Shapiro, R. H.; Lipton, M. F.; Kolonko, K. J.; Buswell, R. L.; Capuano, L. A. *Tetrahedron Lett.* **1975**, *22*, 1811.
(16) (a) Corey, E. J.; Enders, D. *Chem. Ber.* **1978**, *111*, 1337, 1362, and references therein. (b) Enders, D.; Schubert, H. *Angew. Chem.* **1984**, *96*, 368, and references therein.
(17) Jung, M. E.; Shaw, T. J. *Tetrahedron Lett.* **1979**, *43*, 4149.
(18) Ludwig, J. W.; Newcomb, M.; Bergbreiter, D. E. *J. Org. Chem.* **1980**, *45*, 4666.
(19) (a) Collum, D. B.; Kahne, D.; Gut, S. A.; DePue, R. T.; Mohamadi, F.; Wanat, R. A.; Clardy, J.; Van Duyne, G. *J. Am. Chem. Soc.* **1984**, *106*, 4865. (b) Wanat, R. A.; Collum, D. B. *J. Am. Chem. Soc.* **1985**, *107*, 2078.
(20) Philips, J. C.; Perianayagam, C. *Tetrahedron Lett.* **1975**, *38*, 3263.
(21) Kofron, W. G.; Yeh, M.-K. *J. Org. Chem.* **1976**, *41*, 439.
(22) Jung, M. E.; Blair, P. A.; Lowe, J. A. *Tetrahedron Lett.* **1976**, *18*, 1439.
(23) Lyle, R. E.; Saavedra, J. E.; Lyle, G. G.; Fribush, H. M.; Marshall, J. L.; Lijinslij, W.; Singer, G. M. *Tetrahedron Lett.* **1976**, *49*, 4431.
(24) Gawley, R. E.; Nagy, T. *Tetrahedron Lett.* **1984**, *25*, 263.
(25) Spencer, T. A.; Leong, C. W. *Tetrahedron Lett.* **1975**, *45*, 3889.
(26) Fraser, R. R.; Dhawan, K. L. *J. Chem. Soc., Chem. Commun.* **1976**, 674.
(27) Gawley, R. E.; Termine, E. J.; Aube, J. *Tetrahedron Lett.* **1980**, *21*, 3115.
(28) Ikeda, K.; Yoshinaga, Y.; Achiva, K.; Sekiya, M. *Chem. Lett.* **1984**, *3*, 369.
(29) Shatzmiller, S.; Lidor, R. *Synthesis* **1983**, 590.
(30) Lidor, R.; Shatzmiller, S. *J. Am. Chem. Soc.* **1981**, *103*, 5916.
(31) Anti-alkylations may occur in special cases; see refs 11, 18, and 30.
(32) Glaser, R.; Streitwieser, A. *J. Am. Chem. Soc.*, **1989**, *111*, 7340.
(33) Glaser, R.; Streitwieser, A. *J. Org. Chem.*, in press.
(34) Glaser, R.; Streitwieser, A., Jr. *J. Am. Chem. Soc.* **1987**, *109*, 1258.
(35) Glaser, R.; Streitwieser, A., Jr. *Pure Appl. Chem.* **1988**, *60*, 195.
(36) Glaser, R.; Streitwieser, A., Jr. *THEOCHEM* **1988**, *163*, 19.
(37) (a) GAUSSIAN 80 UCSF: Singh, U. C.; Kollman, P. *QCPE Bull.* **1982**, *2*, 17. (b) Binkley, J. S.; Frisch, M.; Raghavachari, K.; DeFrees, D.; Schlegel, B.; Whiteside, R.; Fluder, E.; Seeger, R.; Pople, J. A. GAUSSIAN 82, Release A Version, Carnegie-Mellon University, 1983.
(38) Schlegel, H. P. *J. Comput. Chem.* **1982**, *3*, 214.
(39) (a) Binkley, J. S.; Pople, J. A.; Hehre, W. J. *J. Am. Chem. Soc.* **1980**, *102*, 939. (b) Gordon, M. S.; Binkley, J. S.; Pople, J. A.; Pietro, W. J.; Hehre, W. J. *J. Am. Chem. Soc.* **1982**, *104*, 2197.
(40) (a) Chandrasekhar, J.; Andrade, J. G.; Schleyer, P. v. R. *J. Am. Chem. Soc.* **1981**, *103*, 5609, and references therein. (b) Spitznagel, G. W.; Clark, T.; Chandrasekhar, J.; Schleyer, P. v. R. *J. Comput. Chem.* **1982**, *3*, 363. (c) Sapse, A.-M.; Kaufmann, E.; Schleyer, P. v. R.; Gleiter, R. *Inorg. Chem.* **1984**, *23*, 1569. (d) Winkelhofer, G.; Janoschek, R.; Fratev, F.; Spitznagel, G. W.; Chandrasekhar, J.; Schleyer, P. v. R. *J. Am. Chem. Soc.* **1985**, *107*, 332. (e) Cremer, D.; Kraka, E. *J. Phys. Chem.* **1986**, *90*, 33, and references therein.
(41) Clark, T.; Chandrasekhar, J.; Spitznagel, G. W.; Schleyer, P. v. R. *J. Comput. Chem.* **1983**, *3*, 294.
(42) (a) Pullman, A.; Berthod, H.; Gresh, H. *Int. J. Quantum Chem.* **1976**, *10*, 59. (b) Hobza, P.; Zahradnik, R. *Chem. Rev.* **1988**, *88*, 871, and references therein.
(43) (a) Pople, J. A.; Schlegel, H. B.; Krishnan, R.; DeFrees, D. J.; Binkley, J. S.; Frisch, M. J.; Whiteside, R. A.; Hout, R. F., Jr.; Hehre, W. J. *Int. J. Quantum Chem.* **1981**, *15*, 269. (b) Francl, M. M.; Pietro, W. J.; Hehre, W. J.; Gordon, M. S.; DeFrees, D. J.; Pople, J. A. *J. Phys. Chem.* **1982**, *77*, 3654. (c) DeFrees, D. J.; McLean, A. D. *J. Chem. Phys.* **1985**, *82*, 333.
(44) (a) Hehre, W. J.; Ditchfield, R.; Pople, J. A. *J. Chem. Phys.* **1972**, *56*, 2257. (b) Hariharan, P. C.; Pople, J. A. *Theor. Chim. Acta* **1973**, *28*, 213. (c) Binkley, J. S.; Gordon, M. S.; DeFrees, D. J.; Pople, J. A. *J. Chem. Phys.* **1982**, *77*, 3654.

Table II. Relative Energies and Activation Barriers[a-c]

molecules[a]		3-21+G		6-31+G*//3-21+G	
A	B	SCF	SCF+ZPC	SCF	SCF+ZPC
4a	**5a**	1.57	1.03	2.59	2.05
6a	**7a**	9.29	9.10	3.20	3.01
6b	**7b**	2.96	2.67	3.07	2.78
8a	**9a**	10.72	9.83	7.04	6.15
8b	**9b**	4.75	4.01	4.85	4.11
4a	**4b**	40.69	38.95	31.62	29.88
4a	**4c**	34.81	33.57	27.88	26.64
5a	**5b**	31.95	30.63	24.88	23.56
5a	**5c**	29.98	28.91	24.33	23.26
4a	**10**	22.84	21.71	26.81	25.68
5a	**10**	21.27	20.72	24.22	23.67
6a	**6b**	−2.44	−2.56	0.08	−0.04
6a	**6c**	10.56	10.09	6.30	5.83
6a	**6d**	17.56	17.41	17.09	16.94
7a	**7b**	−8.76	−8.82	−0.05	−0.11
7a	**7c**	11.74	10.90	8.30	7.46
7a	**7d**	7.36	6.63	12.96	12.23
7a	**7f**	5.98	5.54	7.77	7.33
7a	**7e**	−4.19	−5.20	6.88	5.87
7a	**7g**	−4.15	−5.13	6.91	5.93
6a	**11**	8.86	8.26	13.61	13.21
7a	**11**	0.47	0.06	10.40	9.99
8a	**8b**	0.16	−0.16	2.13	1.81
9a	**9b**	5.81	5.64	0.05	−0.12

[a] In kcal mol^{-1}. The energies are given without (SCF) and with (SCF+ZPE) inclusion of the scaled (factor 0.9) vibrational zero-point energy corrections. [b] Values specify the energy by which molecule A is more stable than molecule B. [c] The first five entries are syn-preference energies.

for the description of lithium. These functions are not necessary for the proper description of the metal cation but would increase the number of empty orbitals at the metal atoms and lead to increased basis set superposition error.[42] The 6-31G* basis set was augmented by diffuse sp shells[41] as in the case of the 3-21G basis set to give the 6-31+G* basis set. At this level relative energies and metal affinities are sufficiently accurate.[40] Unless otherwise noted, relative energies given in the text and in the figures are those determined at RHF/6-31+G*//RHF/3-21+G and including vibrational zero-point energy corrections determined at RHF/3-21+G.

Results and Discussion

Equilibrium Structures of Ion Pairs of Oxime Carbanions. To facilitate comparisons, the structures of the acetaldoxime anion are numbered as in ref 33, **4a–c** (syn) and **5a–c** (anti). The number indicates the CN configuration and the letters specify the CC conformation. **4a** and **5a** are planar minima and the others are transition-state structures for CC rotation. In **4b** and **5b** the C_σ lone pair and the CN bond are cis, and they are trans in **4c** and **5c**. The lithium ion pairs (LiIP) **6** (syn) and **7** (anti) and the sodium ion pairs (NaIP) **8** and **9** (vide infra) are numbered as in ref 35, and, as with the anions, letters will be used to further differentiate between these stationary structures. The transition-state structures for syn/anti isomerization of the isolated anion and of the LiIP are numbered **10** (**6** in ref 32) and **11**, respectively.

All minima of the lithium and sodium ion pairs are chiral (C_1).[34,35] For each of the ion pairs formed by the syn- or the anti-configured carbanions, two topologically different minima have been located. The metal cation engages in either a formal η^4- (syn) or η^3- (anti) face coordination, or it bridges the NO bond in a η^2 fashion. The LiIPs of the syn- (**6a**, η^4-face coordination; **6b**, η^2-bond coordination) and the anti-configured carbanions (**7a**, η^3-face coordination; **7b**, η^2-bond coordination), and the corresponding NaIPs, syn, **8a** (face coordination) and **8b** (NO-bond coordination), and anti isomers, **9a** (face coordination) and **9b** (NO-bond coordination), have been discussed previously.[34,35] Structural details and vibrational frequencies for all of these molecules are contained in the supplementary material of this article, and selected data for the NaIPs are included in the tables for ease of comparison.

The LiIPs formed with the same geometrical isomer of the acetaldoxime carbanion but with different hapticities are essentially isoenergetic (Tables I and II). The two NaIPs formed with the anti anion, **9a** and **9b**, are isoenergetic as well. Only the NaIPs of the syn anion show an isomer preference; the formally face-coordinated NaIP **8a** is favored over **8b** by 1.8 kcal mol^{-1}.

Table III. Metal Affinities[a,b]

			3-21+G		6-31+G*//3-21+G	
A	B	M	SCF	SCF+ZPC	SCF	SCF+ZPC
6a	**4a**	Li^+	168.0	165.9	162.5	160.4
6b	**4a**	Li^+	170.6	168.6	162.4	160.4
7a	**5a**	Li^+	160.3	157.8	161.9	159.7
7b	**5a**	Li^+	169.0	166.6	162.0	159.6
8a	**4a**	Na^+	157.1	154.9	135.4	133.5
8b	**4a**	Na^+	157.0	155.1	133.3	131.4
9a	**5a**	Na^+	148.0	146.1	131.0	129.1
9b	**5a**	Na^+	153.8	152.0	131.0	129.3

[a] As in Table II. [b] The affinities for the formation of ion pair A by ion association of anion B with metal cation M^+ in kcal mol^{-1}.

Replacement of the hydroxy by an alkoxy group is not expected to affect the face-coordinated ion pairs to a great extent because the hydroxy group is directed away from the rest of the molecule; however, the orientation of the OH group in the η^2-NO-bond coordinated isomers suggests that these would certainly be affected by such a change. The alkoxy group would also undoubtedly destabilize the NaIPs **8b** and **9b** for similar steric reasons. In the case of the syn-configured ion pair, the alkoxy group may cause the NO-bridged structure to vanish as a local minimum. The structures suggest that the NO-bridged lithium ion pairs are comparatively less subject to steric destabilization. In any case, it appears reasonable to assume that the ion pairs involving face coordination are energetically favored over η^2-NO-bond coordinated ion pairs for metalated oxime ethers. The syn-preference energies (SPE) would then refer to the face-coordinated ion pairs. The SPE is 2.0 kcal mol^{-1} for the acetaldoxime carbanions. Ion-pair formation increases the SPE to 3.0 kcal mol^{-1} for Li^+ and to 6.2 kcal mol^{-1} for Na^+ (Table II). Based on these theoretical results we have suggested that an increased regioselectivity might be achieved by use of bases with larger cations.[34,35] The large metal affinities (Table III) emphasize that the metalated intermediates are best described as ion pairs.

Several other stationary structures have now been located for the LiIPs of the acetaldoxime carbanions, **6c** and **6d** (syn), **7c–g** (anti), and **11**. These structures are involved in the discussions to follow regarding the isomerization between face- and NO-bond coordinated ion pairs (coordination isomerization), the interconversion of enantiomeric ion pairs (racemization), and syn/anti isomerization (geometrical isomerization).

General Stereochemical Considerations. a. Stereochemistry of the Lithium Ion Pairs. To fully appreciate the chirality of the equilibrium ion-pair structures, *two* basic elements of chirality have to be considered.[45,46] The basic element of chirality is the nonplanar arrangement of any four different atoms; three atoms define the reference plane and the fourth atom can be either above or below this reference plane. One of these elements originates from the chirality of the environment of the nitrogen atom. The other results from the relative position of the cation with regard to the NCC plane. The configuration with respect to this second element of chirality can be assigned in the Cahn–Ingold–Prelog system according to the rules for planar-chiral molecules.[47,48] With the cation as the *pilot atom*, the configuration of the planar-chiral ion pairs is *R* or *S* depending on whether the atoms

(45) The term *elements of chirality* is used to describe the stereogenic character of the environment of an atom (N and the gegenion). Mislow and Siegel have stressed *that the purely stereogenic character of elements of chirality of a molecule must not be confused with the chirality properties of that molecule* (ref 46).

(46) Mislow, K.; Siegel, J. *J. Am. Chem. Soc.* **1984**, *106*, 3319.

(47) (a) Cahn, R. S.; Ingold, C. K.; Prelog, V. *Angew. Chem., Int. Ed. Engl.* **1966**, *5*, 385. (b) Prelog, V.; Helmchen, G. *Angew. Chem., Int. Ed. Engl.* **1982**, *21*, 567.

(48) Kagan, H. B. *Organische Stereochemie*; Georg Thieme Verlag: Stuttgart, 1977; pp 107–118.

Scheme I

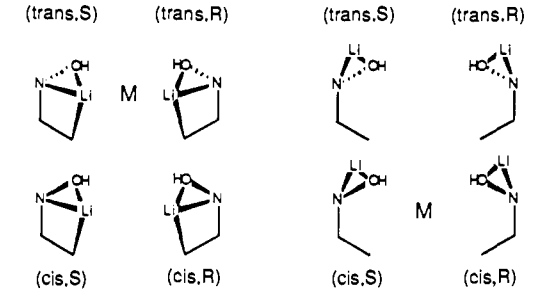

Scheme II

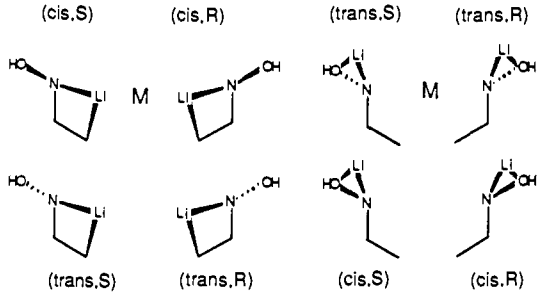

of the *reference plane* (priorities: N > C(N) > C(C)) are arranged in a clockwise (*R*) or in a counterclockwise fasion (*S*) as seen from the pilot atom.[49] Alternatively, this element of chirality could be described in terms of the concept of *cyclic directionality* recently introduced by Mislow[50] or with the rechts-links nomenclature of Ruch based on the signs of homochirality polynominals.[51] The configuration of the asymmetric nitrogen may be described in the conventional way considering the relative positions and priorities of the four substituents. Here, any structure for which the N configuration is such that the oxygen and the gegenion are on the same side of the NCC plane is referred to as the cis isomer and vice versa to clearly differentiate between the two elements of chirality.

The presence of two elements of chirality results in four a priori possible stereoisomers for each of the LiIPs as depicted in Schemes I (syn) and II (anti). Those for which a potential energy minimum actually exists are marked by M (for minimum). Of the eight possible stereoisomers of the syn-LiIP shown in Scheme I, only four exist as stationary structures. The two basic elements of chirality can be considered as being *configurationally correlated* in these structures; that is, the configuration with respect to one of the elements of chirality dictates the other. Similarly, only the enantiomers (cis,*S*) and (cis,*R*) exist for **7a** and only the enantiomers (trans,*S*) and (trans,*R*) of **7b** are minima.

The use of two descriptors for the ion pairs is primarily relevant for the discussion of the ion-pair dynamics, but it also is useful for comparisons among the equilibrium structures. We have previously pointed out an effect of the cation on ion pairs of type **7a**. The lithium derivative **7a** and its sodium analogue **9a** differ with respect to the position of the HO group relative to the NCC plane, and an explanation has been proposed.[34] The HO group in **7a** is bent toward Li^+ whereas it is bent away from Na^+ in **9a**. Hence, the homochiral[51] structures of **7a** and of **9a** are related to each other as "epimers". Similarly, the face-coordinated syn-NaIPs are cis-configured, whereas the corresponding LiIPs are trans-configured.

For all of the ion pairs the equilibrium structures are fully described by either one of the chiral descriptors. However, failure to recognize that (a pair of) enantiomeric structures may contain more than one basic element of chirality prevents the consideration of all possible pathways for their racemization. In particular, one might assume that equilibration between two enantiomers (*R* and *S*) proceeds through an achiral transition-state structure. This assumption is valid only if there is exactly one element of chirality present (vide infra). If there are more than one element of chirality, then chiral transition states to racemization with lower energies may exist. Hence, optimization of all possible achiral structures without characterization of the nature of these stationary points on the potential energy surface is not sufficient to determine the activation barrier for racemization of enantiomers that have more than one basic element of chirality.

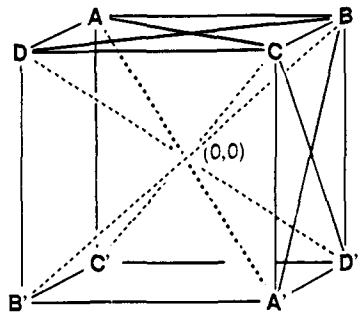

Figure 1. Inversion-symmetric cube graph illustrating the eight-minima isomerization problem. The epimers A and B of one coordination isomer and the epimers C and D of the other coordination isomer define one face of the square. Each line between any of the minima (not all are drawn) represents one a priori possible pathway for one-step isomerization. Possible pathways for one-step racemization are shown as dotted lines; they may or may not involve one of the possible achiral (0,0) structures.

In the following, the a priori possible isomerizations are considered for a molecule that contains two elements of chirality and that can form two coordination isomers. The LiIPs of acetaldoxime represent a special case of this more general scenario. This system is compared to the case that involves only one element of chirality.

b. The Isomerization Problem. The consideration of all of the various possible pathways for coordination isomerization, epimerization, and racemization of two structure isomers that each contain two elements of chirality is in general an eight-minima problem. Such a scenario may be schematically presented by the cube graph shown in Figure 1. The epimers A and B of the first coordination isomer and the epimers C and D of the second coordination isomer (in any order) define the corners of the top square. The enantiomers A′, B′, C′, and D′ define the bottom square, and they are located in such a way as to give the largest possible distance with their enantiomers. Each line between any two of the minima represents one a priori possible one-step isomerization. The pathways can be represented schematically as straight lines with the transition state in the middle. Of these a priori possible isomerizations only those are physically defined for which at least one transition-state structure exists. The chemically significant isomerization pathway between any pair of isomers is that one-step or multistep pathway with the lowest barrier.

c. Racemization via Chiral Transition States. The cube graph retains one important property of the isomerization processes, namely, that any two isomerization pathways that connect either the minima X and Y or their enantiomers X′ and Y′ are enantiomerically related.[52] This condition is the only intrinsic restriction imposed on any pair of isomerizations X $\rightleftharpoons$ Y and X′ $\rightleftharpoons$ Y′. It is trivial that any pair of enantiomerically related coordination isomerizations and epimerizations *cannot* follow *identical* pathways and the transition states for these processes *must be chiral*. In this scenario, a racemization differs from the

(49) For the ion pairs the choice of the pilot atom is not rigorous, and, even if it were, the choice of the reference plane remains arbitrary. Some of these problems are addressed in the supplementary material. In the absence of established rules, we recommend that stereochemical assignments of related compounds be explained carefully in publications.

(50) Mislow, K. *Chimia* **1986**, *40*, 395.

(51) (a) Ruch, E. *Acc. Chem. Res.* **1972**, *5*, 49. (b) Ruch, E. *Angew. Chem., Int. Ed. Engl.* **1977**, *16*, 65.

(52) The inversion symmetry requirement marks a conceptional difference between the cube graph discussed here and other graphs (e.g.: Biali, S. E.; Buda, A. B. *J. Org. Chem.* **1988**, *53*, 135. Gust, D.; Mislow, K. *J. Am. Chem. Soc.* **1973**, *95*, 1535) that have been used to illustrate isomerization processes.

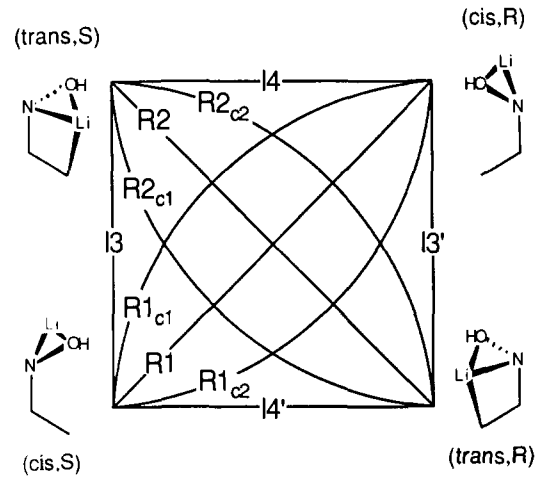

Figure 2. Schematic representation of possible pathways to coordination isomerization (I) and racemization (R) of the syn-configured ion pair. See text.

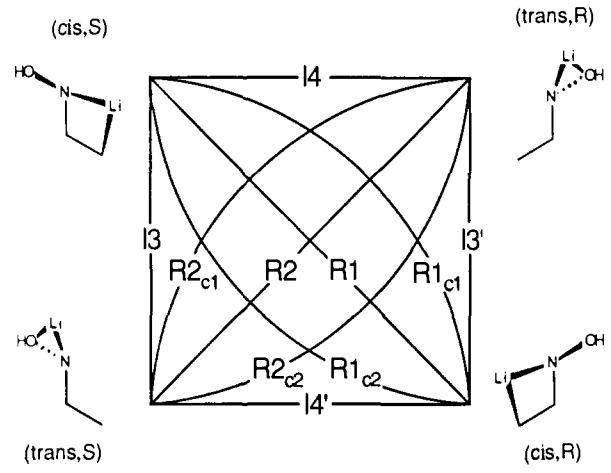

Figure 3. Schematic representation of possible pathways to coordination isomerization (I) and racemization (R) of the anti-configured ion pair. See text.

other kinds of isomerizations intrinsically in that the starting and the end point of the pair of racemization pathways coincide.[53] Hence, the enantiomerically related racemization pathways have *the potential* to become identical, but there is no intrinsic reason why they should.[54-57]

Mislow apparently first pointed out the possibility of totally chiral pathways for racemization.[58] Salem et al.[59] have described the differences between the enantiomerically related pathways and that pathway that involves a symmetric structure for narcissistic reactions in general. Burwell and Pearson,[60] and Wolfe, et al.[61] have shown that such interconversion along two separate pathways are perfectly compatible with the principle of microscopic reversibility.

Thus, chiral transition states for racemization should be common but apparently are not; that is, most enantiomerizations in practice appear to involve transition-state structures that are achiral. One may question why this should be so.

d. Asymmetric Nitrogen and Carbon Atoms. Racemization of molecules with one and only one basic element of chirality do proceed *via* achiral transition states. Racemization of a chiral four-atom system requires the fourth atom to change sides, and, of course, the fourth atom must be coplanar with the three other atoms somewhere along the racemization pathway. This achiral structure must be common to both of the enantiomerically related pathways and, hence, these pathways must be identical. Unfortunately, the identification of all of the basic elements of chirality is obscured in some cases by nomenclature. Only the *asymmetric N atom* in an amine describes a single element of chirality, whereas the *asymmetric C atom* inherently contains *two* basic elements of chirality. Ammonia derivatives Nabc (e.g., NHDT) contain exactly one element of chirality, and their racemization always proceeds *via* achiral transition states. Methane derivatives Cabcd (e.g., CFClBrI) contain two basic elements of chirality; if the fragment Cab is taken as the reference plane, then both of the substituents "c" and "d" can, in principle, be above or below the reference plane. In "normal" structures "c" and "d" are on different sides and one descriptor suffices to classify such stable structures.[62] In complete analogy to the lithium ion pairs, however, the consideration of both of these basic elements of chirality is required in the discussion of the racemization pathways. The racemization of an "asymmetric carbon atom" could involve entirely chiral pathways!

e. Characterization of (0,0) Structures. Both of the syn- and the anti-configured LiIPs give rise to two coordination-isomeric pairs of enantiomers. The coordination isomerization and the racemization processes for each of these ion pairs can be described by the square ACA′C′ of the more general scenario illustrated by the cube graph (Figure 1), and the syn/anti isomerization can be treated separately. The pathways for coordination isomerizations and racemizations are shown schematically in Figures 2 and 3. The search for the transition states can be carried out in a systematic manner starting from all stationary *achiral* (0,0) structures, that is, structures in which both elements of chirality are inactive. First, all plausible C_s-symmetric (0,0) structures are optimized and characterized by normal mode analysis and three cases may then be differentiated.

If a (0,0) structure represents a transition-state structure, then it must be a transition state for racemization and the transition vector shows whether it belongs to pathway R1 or R2 (Figures 2 and 3). (There may be several $(0,0)^{\ddagger}$ structures that connect either of the enantiomers.) The imaginary normal mode is necessarily antisymmetric with respect to the symmetry plane; that is, the infinitesimal displacements of all atoms as specified by the transition vector leads to a molecular distortion that does not preserve the symmetry plane (xz). The transition vector is further restricted in that the x- and z-displacements must have opposite signs for atoms that are symmetrically located with respect to the symmetry plane.[63] In particular, this condition requires the in-plane displacements of atoms in the symmetry plane to be zero. Suppose this statement, the so-called IPD condition (in-plane displacement condition) were not true and an infinitesimal displacement of all of the atoms would be carried out in the direction specified by the transition vector and in the opposite direction. Clearly, the resulting structures would not be enantiomerically

(53) Enantiomerically related pathways have the potential to become identical for *any* isomerization if the starting and the end points of the pathways coincide. In the scenario considered here only racemizations satisfy this requirement.

(54) McIver, J. W., Jr. *Acc. Chem. Res.* **1974**, *7*, 72.

(55) Stanton, R. E.; McIver, J. W., Jr. *J. Am. Chem. Soc.* **1975**, *97*, 3632.

(56) Pechukas, P. *J. Phys. Chem.* **1976**, *64*, 1516.

(57) Nourse, J. G. *J. Am. Chem. Soc.* **1980**, *102*, 4883.

(58) Mislow, K. *Introduction to Stereochemistry*; W. A. Benjamin: New York, 1966; p 93.

(59) (a) Salem, L. *Acc. Chem. Res.* **1972**, *4*, 322. (b) Salem, L.; Durup, J.; Bergeron, G.; Cazes, D.; Chapuisat, X.; Kagan, H. *J. Am. Chem. Soc.* **1970**, *92*, 4472.

(60) Burwell, R. L.; Pearson, R. G. *J. Phys. Chem.* **1966**, *70*, 300.

(61) Wolfe, S.; Schlegel, H. B.; Csizmadia, I. G.; Bernardi, F. *J. Am. Chem. Soc.* **1975**, *97*, 2020.

(62) Mislow and Siegel state (ref 46) that the relationship between enantiomers of the type CHBrClF may be expressed by reference to *any* chirotopic point in the model (as opposed to only the central atom). Each of the five atoms is given its own chirotopic descriptor, that is, an index that describes the sense of chirality defined by the environment of that atom. It was stated implicitly that the index α of H, for example, fully expresses the stereochemical identity of one of the enantiomers. This statement is analogous to our conclusion that only one of the configurationally correlated elements of chirality needs to be considered to describe the identity of a stable enantiomer.

(63) Note that the x and z coordinates are "symmetric" and the z coordinate is "antisymmetric" in the sense of the definition suggested by Salem et al. (ref 59).

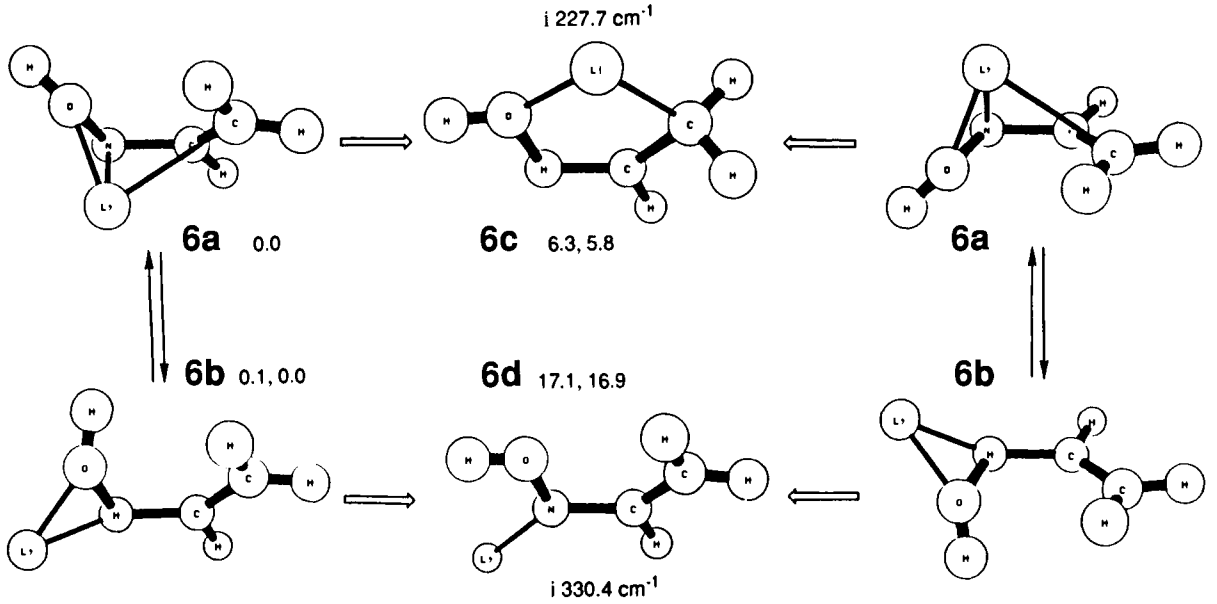

Figure 4. Coordination isomerization and racemization of the lithium ion pairs formed with the syn-configured carbanion of acetaldoxime. Imaginary frequencies are given for structures that correspond to saddle points on the potential energy surface.

related. Hence, the transition vector of an achiral transition-state structure for racemization is antisymmetric and the atomic displacements are restricted by the IPD condition.

If the (0,0) structure is a second-order saddle-point, SOSP $(0,0)^{\ddagger\ddagger}$, then there are two possibilities depending on the characteristics of the imaginary (antisymmetric) normal modes. These modes indicate the distortions necessary to reach the two pairs of enantiomeric stationary points with fewer imaginary frequencies. The information whether the SOSP is connected with two pairs of enantiomeric transition states *or* with one such pair and two enantiomeric minima is contained in the symmetry properties of the imaginary modes. If one of the imaginary modes fulfills the IPD condition, then there must be two enantiomeric transition states for one-step racemization between a pair of enantiomers (pathways $R1_c$ and $R2_c$). The imaginary mode of vibration that fulfills the IPD condition shows which two enantiomers are connected, and the displacement vector of the other imaginary mode indicates how the $(0,0)^{\ddagger\ddagger}$ structure needs to be distorted in the search for the chiral transition states for racemization. If none of the imaginary modes fulfills the IPD condition, then the $(0,0)^{\ddagger\ddagger}$ structure must be connected with the two pairs of enantiomeric transition states through which coordination isomerizations proceed (pathways I3/I3′ and I4/I4′).

Racemization and Coordination Isomerization of the Lithium Ion Pairs. a. Selection of (0,0) Structures. The simultaneous double inversion may either proceed *without* or *with* concomitant rotation of the CH_2 group. The pseudo-π system in the anion persists during racemization without CH_2 rotation (π-type (0,0) structure), whereas concomitant CH_2 rotation involves a (0,0) structure in which the C_σ lone pair of the pyramidalized CH_2 group lies in the symmetry plane (σ-type (0,0) structure). The most reasonable pathways have been explored for each of these types of (0,0) structures for the syn- and for the anti-configured ion pairs. For the racemization of **6a** and **7a**, for example, only those σ-type (0,0) structures in which lithium occupies a bridging position between the CH_2 carbon and one of the heteroatoms appear reasonable. Structures in which the gegenion is coordinated solely to the C lone pair, the metal derivatives of the anions **4c** and **5c**, clearly are energetically disfavored. The racemization of **6b** and the racemization or isomerization of **7a** and **7b** involving π-type (0,0) structures require the lithium to move around the nitrogen and involve structures that are best described as lithiated vinylhydroxyamides. In principle, these (0,0) structures can have either an NO-s-cis or NO-s-trans conformation. The structure with the s-cis conformation appears disfavored for steric reasons for the syn-configured ion pair and, in particular, for the metalated oxime ethers which are being modeled.

Table IV. Selected Bond Distances Involving the Gegenion in the Ion Pairs[a]

ion pair	M–C(C)	M–C(N)	M–N	M–O
6a	2.502	2.254	1.979	1.781
6b	3.986	3.082	1.818	1.789
6c	2.032	2.661	2.744	1.813
6d	4.126	2.846	1.788	2.927
7a	2.270	2.198	1.871	3.058
7b	4.047	3.029	1.822	1.798
7c	2.053	2.374	1.994	3.387
7d	3.103	2.764	1.794	3.025
7f	2.741	2.550	1.794	3.105
7e	4.146	3.179	1.803	1.771
7g	4.146	3.179	1.803	1.770
8a	3.051	2.634	2.138	2.018
8b	4.357	3.377	2.029	2.032
9a	2.591	2.544	2.029	3.419
9b	4.346	3.356	2.029	2.039
11	4.175	3.082	1.816	1.776

[a] In angstrøms.

The structures **6c** and **6d** shown in Figure 4 are the most reasonable achiral structures for the syn LiIP. Both of these structures could be regarded as possible (0,0) structures for the enantiomerizations of **6a** or **6b**. It is obvious that the racemization of **6b** via **6c** would be preceded by the isomerization **6a** ⇄ **6b**. The interconversion between **6a** and **6b** is undoubtedly a fast process; only a small movement of the gegenion is required and the important metal heteroatom contacts are maintained along the isomerization pathway. **6c** (**6d**) thus appears as the only reasonable (0,0) structure for racemization of **6a** (**6b**). The most reasonable achiral structures for the anti LiIP are the structures **7c**, **7d**, and **7e** (Figure 5). The structures **7c** and **7e** are clearly most relevant for the enantiomerizations of **7a** or **7b**, respectively. The structure **7d** appears to be connected to **7a** and **7b**, and **7d** could play a role for the racemization of either structure or even for the isomerization of the two.

All of these achiral structures have been optimized (Tables IV and V) and characterized by analytical calculation of the Hessian matrix. It is found that **6c**, **6d**, and **7c** are transition-state structures, whereas **7d** and **7e** are second-order saddle points (SOSP) on the potential energy surface.

b. Racemization via Achiral σ-Type Transition States. The lithium assumes 1,4-(C,O)-σ- and 1,3-(C,N)-σ-bridging positions in the C_s-symmetric transition-state structures **6c** (syn) and **7c** (anti), respectively. The charge localization in the carbanions

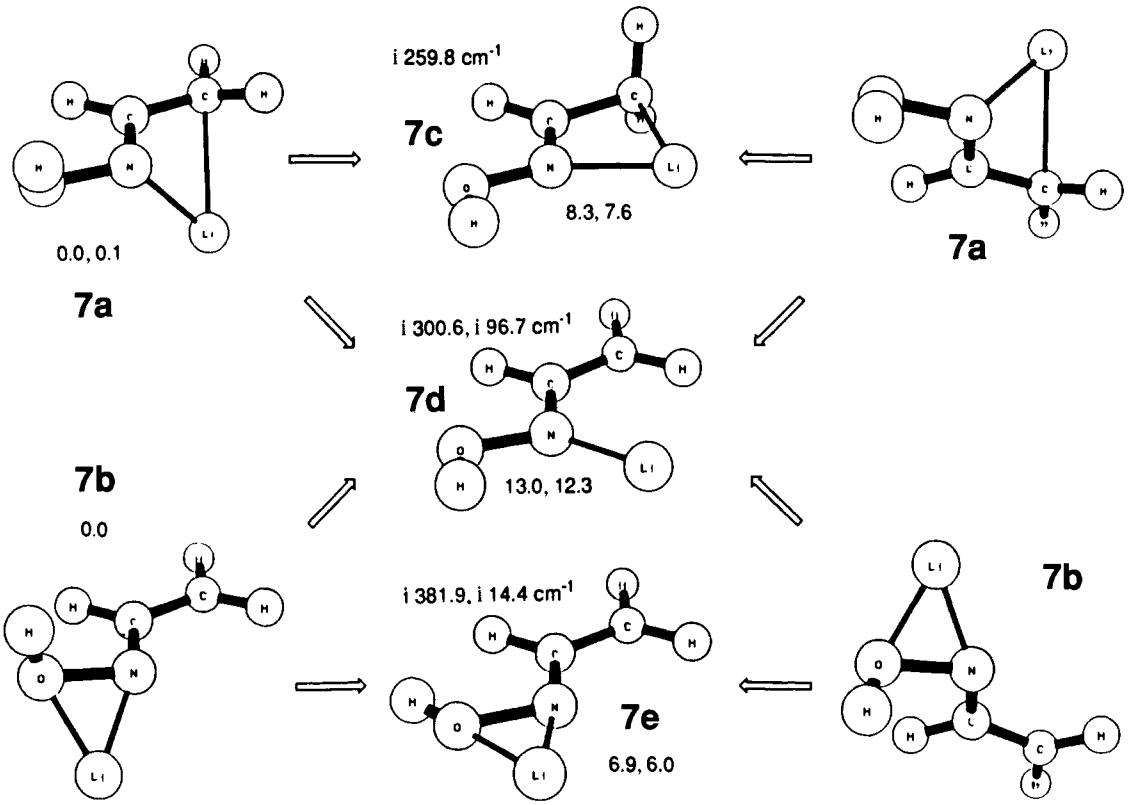

Figure 5. The most reasonable (0,0) structures relevant for racemization of the lithium ion pairs formed with the anti-configured carbanion of acetaldoxime. Imaginary frequencies are given for structures that correspond to saddle points.

Table V. Structures of Stationary Saddle Points of the Lithium Ion Pair of Acetaldoxime

parameter[a]	6c	6d	7c	7d	7f[b]	7e	7g[c]	11[b]
H–O	0.963	0.965	0.967	0.965	0.967	0.964	0.964	0.964
O–N	1.514	1.493	1.459	1.496	1.477	1.591	1.592	1.612
N–C	1.274	1.382	1.276	1.374	1.370	1.382	1.382	1.437
C–*C*	1.502	1.334	1.511	1.343	1.351	1.336	1.335	1.323
C–H_s		1.070		1.081	1.081	1.074	1.074	1.075
C–H_a	1.093	1.074	1.090	1.071	1.072	1.072	1.072	1.074
C–H	1.082	1.082	1.082	1.076	1.078	1.078	1.078	1.081
Li–*C*	2.032	2.867	2.053	3.123	2.741	4.146	4.146	4.175
Li–O	1.813	2.927	3.387	3.025	3.105	1.771	1.770	1.776
Li–N	2.744	1.788	1.994	1.794	1.794	1.803	1.803	1.816
H–O–N	103.4	106.6	105.7	106.3	106.6	115.3	115.3	109.5
O–N–C	110.9	106.7	112.5	105.6	109.6	110.4	110.4	106.7
N–C–*C*	129.3	130.3	116.0	125.3	122.5	124.6	124.6	124.3
N–C–H	108.7	110.7	118.0	106.3	117.0	116.6	116.6	116.2
C–*C*–H_s		121.5		122.9	121.9	122.1	122.0	121.6
C–*C*–H_a	107.8	119.9	109.4	120.9	121.3	120.2	120.2	121.3
Li–*C*–C	96.6		82.0					
Li–N–C		127.3		120.9	106.6	172.9	107.1	142.4
H_s–C–C–N		0.0		0.0	−17.5	0.0	1.4	−0.8
H_a–*C*–C–N	122.8	180.0	121.0	180.0	170.6	180.0	181.6	179.3

[a] In Å and deg. The deprotonated carbon atom is italicized. [b] See text and appendix for further details of **7f** and **11**. [c] Dihedral angles of **7g** (X connected to N and positioned in the HCC plane cis to the CH_2 group): ONCC = 184.1°, HONC = −1.3°, HCNC = 181.1°, LiNXC(N) = 179.3°.

causes the CN and the CC bonds to become close to typical double and single bonds (Table V), respectively. The LiC contacts, relatively unimportant in **6a** and **7a**, are significantly enhanced in **6c** and **7c** (Table V). The interaction between Li^+ and the heteroatom is also enhanced because a σ lone pair of the heteroatom is oriented toward the gegenion and despite the increased bond lengths between Li^+ and oxygen (Δ(LiO) = 0.03 Å) or between Li^+ and nitrogen (Δ(LiN) = 0.12 Å).

The activation barriers are relatively low. The activation energies for racemization (*trans,S*)-**6a** $\rightleftarrows$ **6c**‡ $\rightleftarrows$ (*trans,R*)-**6a** (R2) and (*cis,S*)-**7a** $\rightleftarrows$ **7c**‡ $\rightleftarrows$ (*cis,R*)-**7a** (R1) are only 5.8 and 7.5 kcal mol^{-1} (Table II), respectively. It is revealing that the activation barrier for racemization of **6a** is less than for **7a**. In **7c** an LiN and a less strong LiC contact are replaced by an equal number of stronger lithium contacts. This replacement of lithium interactions effectively counters much of the loss of the pseudo-π delocalization. The reorganization from **6a** to **6c** formally involves the replacement of three lithium contacts in **6a** by only two in **6d**. If the LiC contact were significant for stabilization of **6a**, one would expect the reversed ordering of the activation energies. The low activation barriers also show that rotation of the CH_2 group is greatly facilitated under ion-pair conditions (Table II).[64]

c. Racemization via Planar π-Type Transition States. Among the planar π-type (0,0) structures, only **6d** is a transition-state structure. The transition vector (i330.4 cm^{-1}) of **6d** fulfills the

(64) A similar difference has been noted previously in the effect of ion pairing on CH_2-group rotation in allyl anion: Clark, T.; Rohde, C.; Schleyer, P. v. R. *Organometallics* **1983**, *2*, 1344. In this case heteroatom coordination is not involved.

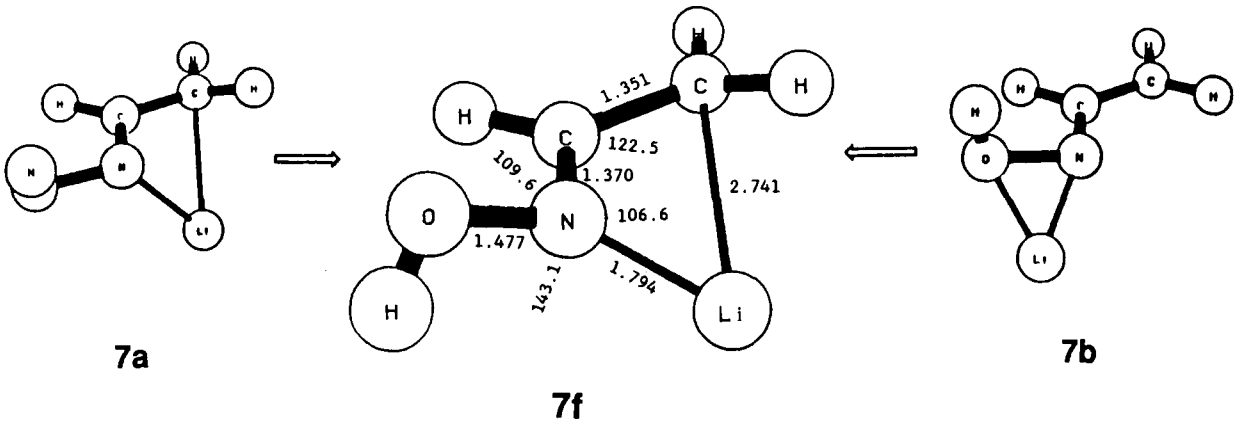

Figure 6. Transition-state structure for the coordination isomerization of the anti-configured lithium ion pair of acetaldoxime carbanion (compare pathways I3 and I3′ in Figure 3). The energy of **7f** relative to **7a** is 7.3 kcal mol^{-1}.

IPD condition and **6d** is the transition state for the racemization of **6b**.

The LiN distances and the geometries of the anions in the ion pairs **6d** and **6b** are essentially identical. The major source for the activation energy **6b** → **6d**‡ is thus the loss of the LiO contact. The activation energy to racemization of **6b** via the pathway R1 is 16.9 kcal mol^{-1} (Table II). The one-step enantiomerization of **6b** thus requires 11.1 kcal mol^{-1} more activation energy than the racemization of **6a**; that is, the direct racemization of **6b** is thus not competitive with the pathway involving two coordination isomerizations (I3 and I3′) and racemization (R2) of the coordination isomer **6a**; (*cis,S*)-**6b** ⇄ (*trans,S*)-**6a** ⇄ (*trans,R*)-**6a** ⇄ (*cis,R*)-**6b**.

d. Racemization and Coordination Isomerization via Chiral Transition States. Both of the imaginary vibrational modes of **7d** do not fulfill the IPD condition. Neither of the transition states that are connected with the SOSP **7d** can therefore be a transition state for one-step racemization. Instead, distortion of the structure **7d** in the direction indicated by one of the imaginary vibrational modes (i300.6 or i96.7 cm^{-1}) will lead to a transition state for the coordination isomerization (pathway I3), and distortion in the opposite direction leads to its enantiomeric transition state (pathway I3′). Similarly, distortion of **7d** in the direction of the second imaginary vibrational mode will lead to the transition-state structure of the pathways I4 and I4′ for coordination isomerization.

One pair of the transition states connected with the SOSP **7d** has been located; the displacement vector of the imaginary vibrational mode (i169.7 cm^{-1}) identifies the enantiomers **7f** as the transition states for the pathways I3 and I3′. The activation barrier for the structure isomerization is 7.3 kcal mol^{-1}. The transition structure **7f** for the coordination isomerization (*cis,S*)-**7a** ⇄ (*trans,S*)-**7b** is shown in Figure 6. The formal η^3-face coordination of **7a** is retained in **7f**. The LiN contact is enhanced and the LiC distance is significantly lengthened in **7f** (Δ(LiN) = 0.077 Å; Δ(LiC$_C$) = 0.471 Å) compared to **7a**. The relative positions of the CH_2 and CH hydrogens are similar for **7a** and **7f**. The CH_2–H_a atoms are moved out of the NCC plane and toward the face of the cation (H_aCCN = 173.6° in **7a** and 170.5° in **7f**), whereas the H_s atoms are moved away from the cation (H_sCCN = 27.1° in **7a** and 17.5° in **7f**). While the transition (*cis,S*)-**7a** ⇄ (*trans,S*)-**7b** is late with respect to the change of the lithium coordination mode, it is early with respect to the cis/trans isomerization. In **7a** lithium and oxygen are on the same side of the NCC plane (ONCC = 4.6°), whereas they are on opposite sides in **7f** (ONCC = 18.0°). The coordination isomerization occurs concomitantly with the rotation of the HO hydrogen around the NO bond. In **7a** and **7b** the HO hydrogen and lithium are on opposite sides of the ONC plane, but they are on the same side in **7f**. The relative positions of this hydrogen in **7a** and **7f** might be taken as an indication that **7f** is actually the transition state for NO-s-cis/s-trans isomerization. However, if this were the case, then there would be no obvious reason for the increase of the LiC distance and the decrease of the LiN distance in **7f** compared to **7a**.

In contrast to the SOSP **7d**, one of the imaginary vibrational modes (i381.9, i14.4 cm^{-1}) of **7e** fulfills the IPD condition. As a consequence, there must be a pair of entirely chiral pathways for the racemization of **7b**. The achiral structure corresponds to a hilltop of the potential energy surface between these enantiomerically related pathways. The adjacent chiral transition-state structure **7g** (i381.3 cm^{-1}) has been located, in the manner described, and it differs only slightly from **7e** (Table V). The largest difference between **7e** and **7g** is found for the ONCC dihedral angle; in **7g** the oxygen is moved out of the NCC plane by 4.1°. The lithium is on the opposite side of the NCC plane (LiNCC dihedral angle = 179.3°), but it is barely moved out of the NCC plane. The configuration of **7g** is thus either (trans,*R*) or (trans,*S*).

The energy difference between the achiral (0,0)‡ structure **7e** and the adjacent chiral transition-state structures **7g** is extremely small. At the level of optimization **7g** is only 0.04 kcal mol^{-1} more stable than **7e**, and the inclusion of the vibrational zero-point energy corrections gives an energy difference of 0.07 kcal mol^{-1}. This energy difference is so small that a distinction between the pathway **7b** ⇄ **7e**‡ ⇄ **7b** (R2) and the pathways **7b** ⇄ (**7g**/**7g**′)‡ ⇄ **7b** ($R2_{c1}$/$R2_{c2}$) becomes practically irrelevant. Yet, the important point to be made with regard to the principles of transition-state theory persists, namely, that the lowest energy pathways of all of the a priori possible one-step pathways for the racemization of **7b** have been found to be chiral.

The structures **7e** and **7g** are elements of the *bifurcating region* of the potential energy surface.[65] The trajectories that connect structures **7b** and pass through the enantiomeric structures **7g** originate at the minima in agreement with the theorem that orthogonal trajectories bifurcate only at stationary points. Valtazanos and Ruedenberg argued that it would *seem unphysical to consider the beginning of the bifurcation at the location of the reactants* in those cases where the distance between the saddle points and the *valley-ridge-inflection point* (VRI) is small compared to the distance between the saddle points and the minima.[65] The second imaginary frequency of **7e** (i14.4 cm^{-1}) is rather small and indicates that the VRI (that is, the point at which the Hessian matrix has one zero eigenvalue and the corresponding eigenvector is perpendicular to the gradient at that point) should be close. Valtazanos, Elbert, and Ruedenberg have found a bifurcating transition-state region on the reaction surface describing the ring-opening reaction of cyclopropylidenes to stereoisomeric allenes.[65,66] In the case of the parent cyclopropylidene, the "stereoisomeric" products are in fact identical; that is, cyclopropylidene and allene are connected by two pathways with chiral transition states.[67] Hence, the racemization of **7b** differs from this scenario only in that product and reactant are enantiomerically related; in this case, not only the transition-state structures but

(65) Valtazanos, P.; Ruedenberg, K. *Theor. Chim. Acta* **1986**, *69*, 281.
(66) Valtazanos, P.; Elbert, S. T.; Ruedenberg, K. *J. Am. Chem. Soc.* **1986**, *108*, 3147.
(67) The chirality in these transition states results because the conrotatory motions of one of the methylene groups is slightly ahead of the other.

Table VI. Geometries of the Planar Second-Order Saddle-Point Structures **7e** at Different Basis Set Levels

parameter[a]	3-21+G	6-31+G*	6-31G*
H–O	0.964	0.947	0.946
O–N	1.591	1.491	1.498
N–C	1.382	1.351	1.354
C–*C*	1.336	1.342	1.335
C–H_s	1.074	1.076	1.076
C–H_a	1.072	1.074	1.074
C–H	1.078	1.083	1.083
Li–O	1.771	1.835	1.827
Li–N	1.803	1.788	1.795
H–O–N	115.3	112.2	111.7
O–N–C	110.4	112.1	112.0
N–C–*C*	124.6	126.5	126.6
N–C–H	116.6	116.2	116.1
C–*C*–H_s	122.1	122.1	122.0
C–*C*–H_a	120.2	119.9	120.1
Li–N–O	62.5	66.4	66.7

[a] In Å and deg. The deprotonated carbon atom is italicized. H_s and H_a are the hydrogens at the deprotonated carbon; H_s (H_a) is oriented toward (away from) N. [b] Frequencies (in cm^{-1}) of imaginary modes (a″): 3-21+G, 381.9 and 14.4; 6-31+G*, 535.6 and 72.3; 6-31G*, 566.7 and 110.1.

the entire pathways are enantiomerically related.[68]

The difference in energy between **7e** and **7g** is so small that the significance of the stereochemical results may be questioned in view of the small basis set used. Of course, even if the results should change with higher theory, the fundamental stereochemical principles presented by this example still remain and should have general applicability to other types of systems. **7e** was optimized at two additional levels, 6-31G* and 6-31+G*. The structural results are presented in Table VI; the principal change is a significant shortening of the ON bond and a concomitant lengthening of the LiO bond. **7e** is still a second-order saddle point at both of these higher levels. The imaginary frequencies (6-31G*: i566.7, i110.1 cm^{-1}; 6-31+G*: i535.6, i72.3 cm^{-1}) are both higher than at 3-21+G indicative of a steeper hill or mound in the potential energy surface. Limitations of computer time did not allow finding **7g** at these higher levels, but the steeper slopes suggest somewhat greater structure and energy changes between **7e** and **7g** than found at 3-21+G.

Structure **7g** (and **7e**) is 6.0 kcal mol^{-1} less stable than the global minimum of the anti LiIP, **7b**. The one-step racemization of **7a** with concomitant rotation of the CH_2 group via **7c** (E_A = 7.6 kcal mol^{-1}) is therefore slightly disfavored compared to the sequence of two coordination isomerizations and racemization (*cis*,*S*)-**7a** ⇄ (*trans*,*S*)-**7b** ⇄ (*trans*,*R*)-**7b** ⇄ (*cis*,*R*)-**7a** for which the highest activation barrier is 7.4 kcal mol^{-1} (**7b** ⇄ **7a**).

Syn/Anti Isomerization of the Lithium Ion Pairs. A rigorous study of the syn/anti isomerization requires the consideration of four pathways, each of which links one of the coordination-isomeric syn LiIPs with one of the coordination-isomeric anti LiIPs. Out of these pathways only one appears reasonable for the following reasons. The dihedral angle ONCC has been found as the principal reaction coordinate for the syn/anti isomerization of the carbanions. This finding may be taken as an indication that the syn/anti isomerization of the ion pair also involves rotation of the hydroxy group around the CN axis. Such an isomerization would be most facile if both the syn and the anti LiIPs being interconverted are NO-bond coordinated ion pairs. The syn/anti isomerization between the enantiomers of the two NO-bond coordinated ion pairs involves two (pairs of enantiomeric) transition-state structures (Figure 7). The gegenion can be either on the same side of the ONC plane (pathways P1 and P1′) or on different sides of the ONC plane (pathways P2 and P2′) in the two structures that are being interconverted.

One of the two transition-state structures has been located and its structure (Table V) is shown in Figure 8. Lithium remains

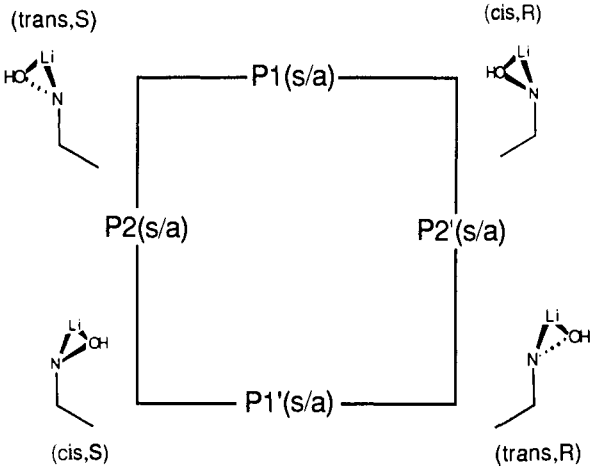

Figure 7. Schematic representation of possible pathways for syn/anti isomerization connecting the enantiomeric η^2-NO-bond coordinated lithium ion pairs of the syn- and the anti-configured carbanions of acetaldoxime.

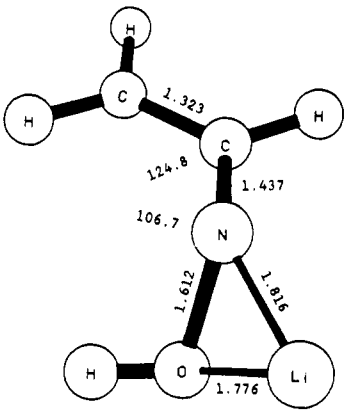

11

Figure 8. Molecular-model-type drawing of one of the transition-state structures for syn/anti isomerization of the lithium ion pair.

η^2-NO-bond coordinated as the syn/anti isomerization progresses by rotation of the HO group around the CN axis. The most remarkable feature of structure **11** concerns the ONCC dihedral angle. On the basis of the Hammond postulate,[69] it might have been expected that the ONCC dihedral angle would be greater than 90°, but the ONCC dihedral angle of **11** is only 75.8°. One explanation for this structural feature would be that there exists another minimum in which the NCC and the ONC planes are more or less perpendicular with respect to each other. Such a minimum has not been discovered. The other explanation does not have to rely on the assumption that there be another minimum. In keeping with the philosophy of considering all of the atomic motions relative to the NCC plane, the syn/anti isomerization involves primarily the movements of the HO group and of lithium. All that the Hammond postulate requires is that the motion of the lithium along the isomerization pathway is more advanced than the motion of the HO group is retarded. This is indeed the case; the lithium and the CH_2 group are on different sides of the plane perpendicular to the NCC plane that contains the CN axis.

The activation energies for the processes **6b** → **11** → **7b** and **7b** → **11** → **6b** are 13.2 and 10.1 kcal mol^{-1}, respectively. These values indicate that connectivity isomerizations and racemizations with or without rotation of the CH_2 group are faster processes than the syn/anti isomerization.

(68) Because the pathways are enantiomerically correlated, the lines tangent to the trajectories at the saddle points are parallel. The "extent of the bifurcating region" can thus not be described as in ref 65.

(69) Hammond, G. S. *Tetrahedron Lett.* **1955**, *77*, 334.

Mechanistic Implications. The structures and the various isomerization pathways of metalated oximes have been discussed for monomeric unsolvated ion pairs. In solution these intermediates are certainly solvated and probably aggregated.[70] However, the characteristics of the monomeric ion pairs are pertinent to any understanding of the structures and reactivity of such metalated species and some aspects are addressed in the following section.

a. Aggregation. The general topological features of the equilibrium structure(s) of monomeric ion pairs carry over in general to the aggregates. The characterization of all possible isomers of the ion pair is thus a prerequisite for the consideration of the aggregated species. In the present case there exist two isoenergetic monomers for the syn and the anti LiIPs, and each could in principle form structurally and energetically different aggregates. Whether aggregation will lead to distinct aggregates or whether one type of aggregate will dominate depends on the activation barrier for coordination isomerization of the monomers. Here it has been shown that the coordination isomerization is facile, and, hence, the one most stable syn or anti aggregate can be formed from either isomer of the syn- or the anti-configured monomer, respectively. Whether the configuration of the anions in the aggregates will be syn or anti depends on the activation barrier for the syn/anti isomerization of the monomers. If dimerization is slower than syn/anti isomerization, then the one most stable aggregate formed by either syn- or anti-configured monomers will be formed, but if dimerization is faster than isomerization, then aggregates with different configurations and different relative stabilities result and the rate of their interconversion will be determined not by the barrier for syn/anti isomerization of the monomer but by the rate of fragmentation of the aggregates. The results presented suggest that *all of the barriers for isomerization of the monomeric ion pair are small enough as to allow the formation of the thermodynamically most favorable aggregate.*

Our semiempirical study of solvated aggregates[36] suggests a cyclic, C_i-symmetric dimer formed by two η^2-NO-bond coordinated syn LiIPs with opposite chirality as the most stable species in solution. Each lithium coordinates to the heteroatoms of one anion in a η^2 fashion, to the CH_2 carbon of the other anion, and tetracoordination of each lithium is achieved by additional primary solvation. The most stable dimer formed by the anti LiIP is also C_i-symmetric, and it is formed by combination of two face-coordinated monomers in such a way that each lithium atom coordinates additionally to the CH_2 group of the other anion and to one solvent molecule. One of the more important findings of the study of the dimers[36] concerns the availability of the CH_2 carbon for addition of an electrophile. The reactive site is more fully coordinated in the dimers compared to the monomers, and at least partial fragmentation of the aggregates would have to occur in order to allow the addition of the electrophile. There is thus no apparent advantage for the reaction of such ion-pair aggregates with an electrophile, and it would appear to be more likely that solvated monomeric ion pairs are the reactive species in solution.[36]

b. Direction of Approach of the Electrophile. There is some controversy as to the preferential side of entry of the electrophile in the reaction with a metalated enolate equivalent of this sort.[19,35] Collum et al. recently proposed a mechanism for the alkylation of closely related hydrazone derivatives;[19] it was argued that the presumed η^4-coordination would preclude entry of the electrophile from the coordinated face (syn entry, Scheme III) and, therefore, would require attack opposite the side of metal coordination (anti entry). However, our theoretical results show that the reacting carbanion is only weakly coordinated to the cation in the face-coordinated ion pair and that the barrier for coordination isomerization is small. Reaction from the face of metal coordination should not be seriously impeded.[71] Indeed, reaction involving

Scheme III

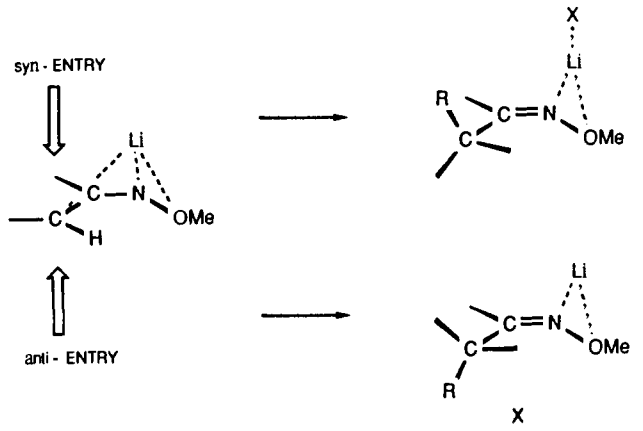

syn entry of the electrophile should be favored over the alternative pathway because precoordination can place the nucleophile of the electrophilic reagent close to the cation of the metalated intermediate and lower the energy of the reaction transition state.[72] We have recently reported that the protonation of the syn LiIP by hydrogen fluoride proceeds only if the electrophilic reagent attacks the metal-coordinated side. In this case precoordination of HF to the gegenion allows orientation of the reagent toward the methylene carbon and proton transfer with concomitant ion-pair formation in the products. Attack of HF from the opposite side does not lead to protonation in this gas-phase model because the gegenion cannot pass through the plane of the anion as HF approaches and ion-pair formation in the products is impeded.[35,73]

c. Metalated Oxime Ethers in Stereoselective Synthesis. Alkylation of configurationally fixed metalated oxime ethers such as 4-*tert*-butylcyclohexanone oxime methyl ether[26] proceed stereoselectively by syn-axial entry of the electrophile.[74] The stereoselectivity results from the preference for chair conformations in the reaction transition-state structures and the stereochemistry does not reflect the syn or anti entry of the electrophile. However, the chirality of the ion pairs together with the face preference of entry of the electrophile could be used to control the stereochemistry at the α-carbon in reactions of other diastereoisomeric metalated oxime ethers. Regioselective syn-deprotonation of an oxime ether with an enantiomerically pure chiral group *E* attached to the oxime O results in a pair of diastereoisomeric metalated intermediates. In order to afford asymmetric induction it would be necessary that there be a sufficient energy difference between the diastereoisomers and that the chiral auxiliary be located close to the reactive center. The latter requirement is especially crucial. The results presented show that displacements of the gegenion are facile; coordination isomerization requires but little energy. *E* groups that contain donor atoms capable of additional coordination to the gegenion appear to be promising candidates if they could be designed in such a way as to assure that face-coordination remains dominant over NO-bond-coordination.[75] Addition of

(70) For an experimental study of aggregation effects, see ref 30. The regioselectivity of the alkylation of 3-methyl-4*H*-5,6-dihydro-1,2-oxazine depends on the steric demands of the base used for deprotonation.

(71) Primary solvation further removes the gegenion from the deprotonated carbon. Ab initio calculations of the ion pairs with inclusion of one water molecule indicate that **6a** and **6b** merge under the influence of one model-solvent molecule. The position of lithium in the solvated LiIP resembles the position of sodium in **8a**. Solvation of **7a** and **7b** has but small effects on structures, but the hydrate of **7b** is slightly more stable than the hydrate of **7a**. The SPE is slightly larger for the monosolvated ion pairs: Glaser, R.; Streitwieser, A., unpublished results.

(72) (a) Beak, P.; Meyers, A. *Acc. Chem. Res.* **1986**, *19*, 356. (b) Meyers, A. *Acc. Chem. Res.* **1978**, *11*, 375.

(73) Cases are known in which protonation and alkylation occur at different sides of a lithium coordinated carbanion; see, for example: (a) Meyers, A. I.; Dickman, D. A. *J. Am. Chem. Soc.* **1987**, *109*, 1263. (b) Nakamura, K.; Higaki, M.; Adachi, S.; Oka, S.; Ohno, A. *J. Org. Chem.* **1987**, *52*, 1414.

(74) For a discussion of the mechanism, see ref 36.

(75) MNDO calculations (constrained optimizations as discussed in ref 36) were carried out of lithiated acetaldoxime 3′-oxabutyl-(1′) ether. In the syn-configured ion pair the oxygen of the side chain coordinates to the gegenion and the methyl group is placed close to the reactive carbon center (unpublished results).

the electrophilic reagent RX to the reactive C center of an α-substituted (R′) oxime ether of this sort could yield predominantly one of the two possible products of opposite configuration at the α-carbon if the face selectivity were sufficiently large. Additional chelation by the donor atom in *E* results in tris-coordination of lithium; precoordination and syn entry of a reagent should not be impeded. The choice of the absolute configuration of the chiral auxiliary could then be used to predictively form CC bonds in a regio- and stereoselective fashion in the α-position of oxime ethers. If the entry of the electrophile occurs indeed in the suggested syn fashion, the approach of a prochiral reagent should be affected by the configuration of the chiral auxiliary, and stereoselective formation of two new asymmetric centers might be achieved.

Conclusions

Coordination isomerizations and racemizations of each of the syn- and the anti-configured ion pairs of acetaldoxime have been discussed in a systematic manner by examination of the number and the symmetries of the imaginary vibrational modes of the achiral (0,0) structures. Achiral structures that are minima would be intermediates for interconversion between any of the adjacent chiral minima. In the present case such achiral minima do not exist; the (0,0) structures are either transition-state structures or second-order saddle points. (0,0) structures with one imaginary frequency are transition-state structures for racemization, and the transition vector identifies the enantiomers that are interconverted. Two kinds of (0,0) second-order saddle points have been found. If none of the imaginary modes fulfills the in-plane displacement (IPD) condition, then the (0,0) structure is connected with two pairs of enantiomeric transition states for coordination isomerization. If one of the imaginary frequencies does fulfill the IPD condition, then there exists a pair of chiral transition states for one-step racemization. The racemization of **7b** provides an example of the latter case.

Ion pairing greatly facilitates rotations around the CC bond and the interconversion between geometrical isomers as compared to the free anions. All isomerizations of the ion pairs are found to have only small activation barriers. Thus, all of the isomeric ion pairs are readily available as building blocks for the thermodynamically most stable aggregates and as intermediates for reactions. Coordination isomerizations and racemizations involve either σ-type transition-state structures (1,4-(C,O)-σ- or 1,3-(N,C)-σ-bridged in the case of the syn- or the anti-configured ion pair, respectively) or transition-state structures in which the gegenion coordinates solely to the N_σ lone pair and the π-conjugation is maintained (π-type transition-state structures). The σ-type transition states involve rotation of the CH_2 group. The replacement of the HO group by an RO group is not expected to impede the rapid isomer interconversion seriously. The activation barrier for the one-step racemization of the NO-bond coordinated anti-configured ion pair would certainly be higher for metalated oxime ethers, but this racemization would still be possible via the pathway involving 2-fold coordination isomerization and racemization of the face-coordinated ion pair. However, alkoxy groups together with an alkyl substituent at the α-carbon should cause significant increases of the activation barriers for racemization. An α-substituent would probably increase the activation barrier for rotation around the CC bond substantially and such racemization pathways of the face-coordinated ion pairs may not be accessible. In these cases racemization via N-coordinated structures of the type **6d** may become important.

The long bond distances between the gegenion and the reactive carbon center and the facile interconversion between coordination isomers of the predominant syn-configured ion pair indicate that the entry of the electrophile from the metal-coordinated side should not be impeded. In contrast, such syn entry is likely to be favored over the anti entry as it allows prior coordination of the electrophile to the cation and ion-pair formation of the product. The chirality of the ion pairs could be exploited for regio- and stereoselective CC-bond formation at the α-carbon. Metalated oxime ethers with an enantiomerically pure chiral auxiliary in the alkoxy group could be used for this purpose if it were possible to design the alkoxy group in such a way as to assure face-coordination in the diastereoisomeric intermediate.

Finally, the solvation of the lithium has not been considered in the computations; however, the various stationary structures found can provide starting points for assessing qualitatively the effects of additional coordination to solvent in real examples in organic synthesis.

Acknowledgment. This research was supported in part by NIH Grant No. GM-30369. The calculations were carried out in part with computer time granted on the Cray II of the San Diego Supercomputer Center supported by NSF and on the VAX-8800 of the UC Berkeley Central Computer Facility. We are also indebted to Prof. S. Shatzmiller for important discussions.

Supplementary Material Available: *Z*-matrix forms, energies, and vibrational frequencies (and transition vectors) of the lithium ion pairs **6a–d** (syn), **7a–f** (anti), and **11** and of the sodium ion pairs **8a** and **8b** (syn) and **9a** and **9b** (anti) (13 pages). Ordering information is given on any current masthead page.

Theoretical Study of C_4O and C_6O

D. W. Ewing

Contribution from the Department of Chemistry, John Carroll University, Cleveland, Ohio 44118. *Received February 13, 1989*

Abstract: Ab initio calculations were performed which corroborate the interpretation of recent ESR data for C_4O and C_6O. Bond lengths, gross orbital spin populations, $^1\Sigma^+ - X^3\Sigma^-$ energy differences, stabilities, dipole moments, and vibrational frequencies were obtained from Hartree–Fock calculations. Electron correlation was included via second-, third-, and fourth-order many-body perturbation theory. Linear geometries were assumed in this study.

The C_4O and C_6O molecules have recently been observed by Van Zee, Smith, and Weltner (VSW) via electron spin resonance (ESR) in neon and argon matricies at 4 K.[1] VSW found these molecules to be triplet linear species with cumulene-like bonding, e.g. :C═C═C═C═Ö:. Also, the zero-field splitting parameter, $|D|$, was found to be larger for C_6O than for C_4O. This is similar to the increase in $|D|$ observed for the series C_4, C_6, and C_8 and was explained in the latter case by increasing spin–orbit contributions to $|D|$, by the first excited $^1\Sigma_g^+$ state, with increasing carbon chain length.[2]

(1) Van Zee, R. J.; Smith, G. R.; Weltner, W., Jr. *J. Am. Chem. Soc.* **1988**, *110*, 609–610.

(2) Van Zee, R. J.; Ferrante, R. F.; Zeringue, K. J.; Weltner, W., Jr.; Ewing, D. W. *J. Chem. Phys.* **1988**, *88*, 3465–3474.

0002-7863/89/1511-8809$01.50/0